Design, Manufacturing and Testing of Composite Type Cylinder Sorghum Thresher

Birhanu Atomsa Gurracho[1*], Abebe Fanta Bedie[2], Yetenayet Bekele Tola[3], Solomon Abera Habtegabriel[4], and Sirawdink Fikreyesus Forsido[3]

[1]Department of Agricultural Engineering, Fadis Agricultural Research Center, Harar, Ethiopia

[2]Department of Agricultural Engineering, Institute of Technology, Haramaya University, Dire Dawa, Ethiopia

[3]Department of Postharvest Management, Jimma University, Jimma, Ethiopia

[4]Department of Postharvest Technology, Institute of Technology, Haramaya University, Haramaya, Ethiopia

Abstract

Background: Sorghum cultivars of widely diverse types of head structures and grain properties are produced in Ethiopia. These require different key threshing actions of various functional elements. But sorghum threshers with cylinder consisting of different functional elements are lacking in the country.

Objective: The study was aimed to design, manufacture, and test the functionality of a sorghum thresher developed with a composite type cylinder using a selected sorghum variety.

Materials and Methods: Fundamental theories, basic principles of design analysis and methods reviewed from the already published research output were followed to design the thresher. The produced prototype was tested at different levels of concave clearance, cylinder speed and feed rate factors laid in $2x3^2$ factorial design with 3 replications using the sorghum variety of *Gubbiye*.

Results: The test results indicated increasing mean threshing efficiency from 96.15% to 99.52%, an average cleaning efficiency of 95.43% and an average unthreshed grain loss of 1.42%. Grand mean of 0.77% grain damage was observed with the means ranging from 0.25% to 1.07%. Grains remained with glumes indicated the highest mean of 4.15% at 400 rpm that was reduced to 2.25% at 600 rpm.

Conclusion: The results revealed an average of 98.58% threshing efficiency, grain damage of 0.77%, and 3.16% grains remaining in glumes from the test made on *Gubbiye* variety. This implies that a designed thresher is efficient which can be used by farmers for threshing grains of sorghum varieties in the country.

Keywords: Composite cylinder; Grain damage; Thresher design; Threshing efficiency; Unthreshed grains

1. Introduction

In Ethiopia, sorghum is a major staple cereal food grain produced in lowland areas (Masresha Fetene *et al*., 2011) with a total production of about 5.02 million tons as indicated by Food and Agricultural Organization (FAO) (2020) engaging more than 5 million farmers according to Central Statistics Authority (CSA) (2020). Regardless of this high production level and its socioeconomic importance to the nation, the production method, particularly the threshing method has remained traditional without noticeable improvement for centuries. A significant portion of sorghum grains produced in the country is lost due to this traditional method, mainly during postharvest activities, particularly during threshing and winnowing. During threshing and cleaning, grains are lost physically because of incomplete threshing, spillage, scattering of grain in the threshing field and grains passing with the chaffs while qualitative losses occur due to breakage of grain, grains remaining with their glumes and contamination with soil dust and dirt spoilage which are also major factors to enhance large deteriorations in the store (Ali Mohammed and Abrham Tadesse, 2018). A recent study of postharvest losses showed 25.81% annual average losses of grain crops in Ethiopia with considerable variation across crop types (Sisay Debebe, 2022). Sorghum postharvest loss assessment conducted in different parts of Ethiopia indicated an average total postharvest loss of 27.40% from which 67.39% was accounted for pre-storage postharvest losses and 7.78% of the total production was threshing and cleaning losses (FAO, 2017). This report has indicated that the traditional farmers' practices of sorghum threshing as problem in postharvest operation and a critical grain loss point in the sorghum postharvest production process of the nation.

Some efforts have been made by different governmental institutions and non-governmental organizations in the last three decades to improve the sorghum threshing method by introducing stationery threshers adapted or modified from threshers originally designed for other cereals like wheat and barley. The threshers locally known as FR-Model thresher, modified IITA multi-crop thresher, Jimma-multi-crop thresher

*Corresponding Author: biratomsa@yahoo.co.uk

ISSN 1993-8195 (Online), ISSN 1992-0407(Print)

with replaceable cylinder and FARC-multi-crop thresher were thresher disseminated by different institutions during last decades and currently in use for threshing of sorghum besides other cereal crops (Samuel Adimasu *et al*., 2014; Husen Abbagisa *et al*., 2015; Takkalign Badada, 2018). All of them are peg types in their cylinder designed majoring a key function of impacting action, though they named as multi-crop threshers (Fu *et al.,* 2018) and lack sufficient components of other key threshing action required for threshing of different crops.

The modified IITA multi-crop thresher of a relatively better performance is the most adopted by farmers, especially in wheat, barley and teff producing areas as reported by SG-2000 (Samuel Adimasu *et al*., 2014). However, the modified IITA multi-crop thresher itself has limitations on sorghum threshing as indicated by high ratio of 9.33% grains remaining with glumes and low threshing efficiency range of 87.89% to 95% reported for *Muyra* sorghum varieties (Ttakkalign Badada, 2018, 2021). This report indicated that even the maximum efficiency of 95% was recorded at high speed of 900 rpm that caused high grain damage on the other way. The FARC Mult-crop thresher improved for sorghum from IITA thresher was also reported for threshing efficiency variation of 88.97% to 97.08% recorded from sorghum produced in different locations by different farmers (Abdulaziz Teha *et al*., 2020) which means low threshing efficiency of less than 95% on most of the sorghum types involved in their study. This drawback could be lack of the required other threshing action components, mainly lack application of sufficient rubbing force which is the important threshing action mostly required in sorghum threshing (Sale *et al*., 2017).

Different crop types require different threshing actions (impacting, cutting, pressing, rubbing, twisting, etc) for the reason that they have different threshing properties based on the inherent characteristics of a particular crop type and/or a specific variety the same crop type (Dhananchezhiyan *et al.,* 2013). Similarly, the cylinder functional elements are designed majoring a key threshing action such that rasped bars are for rubbing action, pegs are for impacting actions, flat spikes are for cutting/shearing action, etc and the selection is determined by the threshing properties of the specific crop type and variety (Fu *et al*., 2018). Sorghum crop produced in Ethiopia are generally characterized by widely diverse types of head structures that ranges from the highly flexible open types to the closed and compact type heads owning highly different threshing properties. Development of a thresher for efficient threshing of these diverse sorghum types requires designing of special threshing cylinder consisting systematic arrangement of various functional elements of different key threshing actions. The objective of this study was thus, to design, manufacture and test functioning of the thresher developed with composite type cylinder using a selected sorghum variety.

2. Materials and Methods

2.1 Description of the Thresher and Working Principle

The thresher was designed for axial threshing system with radial feed inlet on one side near the axial end of the cylinder and radial straw outlet on the opposite side near the other axial end of the cylinder. The crop materials entered at the inlet moves spirally in the threshing chamber while the grains are threshed by repeated actions of different functional elements before reaching the outlet and thrown out. The threshed grains pass through the concave holes and flow across the air stream blown under the concave to removes the chaffs and other light impurities from the grains. The grains dropped on the slopping pan slide and flow to the output collection floor. The thresher has provision for concave adjustment and sliding engine seat to loosen and tighten the belt.

The main parts of the designed and manufactured thresher include the threshing cylinder, the concave, the upper and bottom covers of threshing chamber, the blower and the main frame for assembling and holding them together. The isometric view of its assembly is shown in Figure.1 without the cover of its upper chamber. The thresher was designed and manufactured in such a way that it can be easily dissembled into parts (Figure 2) and can be moved to wherever needed and assembled by any user. There is all also a detachable wheel system developed for moving the thresher on the farm. Hence, it can be transported from farm to farm or village to village in rural areas either by draught animals or by human labour, easily.

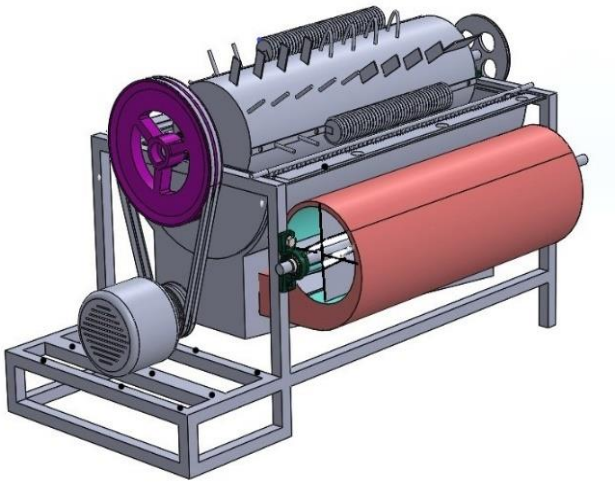

Figure 1. An isometric view of the designed thresher without upper chamber cover.

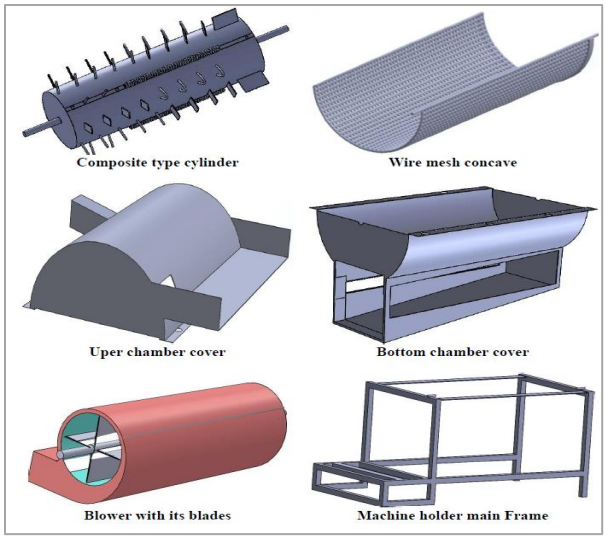

Figure 2. Main component parts of the thresher designed with composite type cylinder.

2.2 Design Analysis

The design began with the establishment of the desired capacity, manageable size and stability during operation, health and safety, availability of construction materials, strength, durability and cost. The capacity of the thresher was decided to be 1.2 t ha^{-1} based on the average yield of 2.69 t ha^{-1} sorghum produced by farmers (CSA, 2021) so that it can serve an average of 3 farmers per day to address more farmers in a given village or Kebele within short seasonal duration before the onset of the small rainy season. It was assumed that a thresher capable of efficiently threshing the heads Gubbiye sorghum variety with the relatively hardest threshing properties can thresh other types of sorghum heads easily. The key threshing actions required to thresh sorghum are impacting, cutting, pressing and rubbing forces (Sale *et al.*, 2017). Based on this assumption, flat spikes, round pegs, wire loop and rasped bars type functional elements were selected to combine functions of the indicated key threshing actions.

2.2.1 Design of threshing cylinder

The length of threshing cylinder is directly related to the feed rate and it was computed with Eqn.1 (El-Sharabasy *et al.*, 2007; Yang *et al.*, 2021).

$$Q = qLR \quad (1)$$

Where, Q = maximum feed rate (kg s^{-1}), q = allowable feed rate per second per meter of cylinder length (kg $s^{-1}m^{-1}$); L = cylinder length (m), and R = number of axial rows of threshing elements on the cylinder surface. Q and q of 0.46 kg s^{-1} and 0.095 kg $s^{-1}m^{-1}$, respectively were computed depending on the intended thresher capacity and average grain to straw ratio of 3.61:1 obtained from data collected for this purpose from 3 varieties of harvested sorghum heads. Six rows of key elements were considered based on the 4 to 8 rows recommendation of Klenin *et al.* (1985) for cylinder of cereals thresher. Inserting these values in Eqn. (1), a cylinder length of 0.80 m was obtained.

The cylinder diameter was determined based on the cylinder rpm and the peripheral velocity required for sorghum threshing as given by Eqn. (2) (Sale *et al.*, 2016; Idris *et al.*, 2018).

$$V_p = \frac{\pi D_p N}{60} \quad (2)$$

The peripheral diameter of the cylinder was calculated using Eqn. (3) (Takkalign Badada, 2018).

$$D_P = (D_c + 2P_h) \quad (3)$$

Where, V_p = peripheral velocity of the cylinder (m/s), D_p = peripheral diameter of the cylinder at the tip of the cylinder elements (m), N = speed of the cylinder (rpm), D_c = diameter of the cylinder at bottom of the pegs (m), and P_h = height of the elements above the closed cylinder surface (m).

Peripheral velocity of 10 to 12 m s^{-1} was suggested for sorghum threshing cylinder by Abich *et al.* (2017) after evaluating at speeds of 8 to 12 m s^{-1}. Indris *et al.* (2018) indicated 10 ms^{-1} speed gave optimum throughput, better efficiency and lower sorghum grain damage. Muhammad *et al.* (2013) recommended tip velocity of 10 m s^{-1} and angular speed of 500 rpm after evaluating sorghum threshers of different diameters.

Considering the velocities recommended by different researchers, 10 m s^{-1} and 500 rpm were selected, and peripheral diameter (D_p) became 0.38 m using Eqn. (3). The height of the cylinder elements above the cylinder surface was determined to be 60.00 mm based on the measured size of compact heads of the *Muyra* and *Gubbiye* sorghum variety. Inserting this value for P_h in Eqn. (3), the diameter of the closed cylinder (D_c) was calculated to be 260.00 mm. The cylinder functional elements were composed of beater pegs, flat spikes and looped wires arranged in six rows of axial direction on the cylinder surface in a systematic order. In addition, three rasped bars, each having a height of 56.00 mm and a length of 300.00 mm were bolted at angular intervals of 120° on the outlet side of the cylinder (Figure 3).

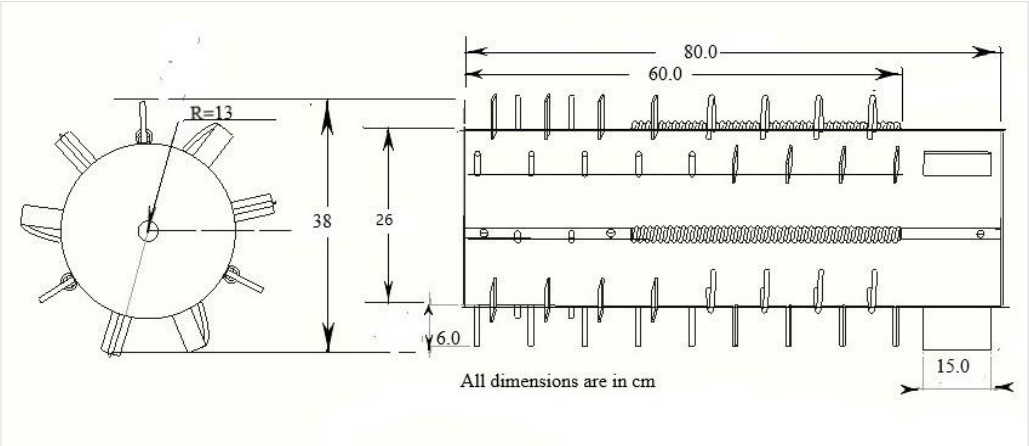

Figure 3. Dimensions of the composite cylinder and arrangement of the key functional elements.

2.2.2 Design of concave

A semi-circular concave was developed from meshing of 4 mm steel wire diameter to cover the bottom half of the threshing cylinder. The concave mesh holes were 6.00 mm x 8.00 mm depending on the maximum mean of sorghum grain major diameter value of 5.65±0.33 mm at moisture content ranging from 10% to 20% (wb) obtained from grain physical and mechanical property measured for 3 varieties with 50 grain samples taken at intervals 2% moisture differences for each variety. The concave diameter determined using Eqn. (4) (Sale *et al.*, 2016).

$$C_d = D_p + 2C_c \quad (4)$$

Where, C_d = concave curvature diameter (m), D_P = diameter of the cylinder at tip of the pegs (m), and C_c = cylinder-concave clearance (m).

A maximum of 30.00 mm uniform concave clearance was considered for the design of the concave to get the sufficient inlet clearance when installed off-centre and also assuming future potential use of the thresher for different crop types of larger grain sizes that resulted in a concave curvature diameter of 440.00 mm using equation (4). The concave was hinged off-centre at 50.00 mm inlet clearance with adjustment system at the outlet side of the cylinder. Two parallel bolts welded on the frame secured the concave outlet side with the provision of two nuts on each bolt used for adjusting the concave clearance between 5.00 and 30.00 mm, whenever needed.

2.2.3 Determination of power requirement

The total power required at the thresher shaft is the sum of all powers required to operate different components and activities performed in threshing the crop. The total power includes powers required to rotate the cylinder, to thresh the crop, to overcome bearing frictions and air resistance to the rotating cylinder as well as the power required to drive the blower. The power needed to drive the unloaded cylinder was computed by Eqn. (5) (Olaoye *et al.*, 2011).

$$P_d = \frac{2\pi N r M_d}{60x75}\left[g + \frac{V_t^2}{r}\right] \quad (5)$$

Where, P_d = power to drive empty cylinder (w), N = cylinder speed (rpm), M_d = total weight of cylinder part with its pulleys (kg), r = effective radius of the rotating mass (m), V_t = cylinder peripheral speed (m s^{-1}), and g = acceleration due to gravity (9.81 m s^{-2}).

The second is the power required to thresh the crop. This power includes the impacting force to detach the grain, the forces to rubbing the crop against the concave and push the crop materials through the chamber, and the force needed to overcome friction of crop to crop and crop to the metal parts. The total of this was given by Eqn. (6) as used by Ali *et al.* (2021).

$$F_c = F_i + F_r \quad (6)$$

Where, F_c = crop threshing force (N), F_i = impact force (N), F_r = crop friction forces (N).

The impacting force depends on the feed rate, the speed of crop materials and crop friction. It was estimated according to Chavoshgoli *et al.* (2019) using Eqns. (7) to (9).

$$F_i = q\,(V_2 - V_1) \quad (7)$$

$$F_r = fF_c \quad (8)$$

$$V_2 = aV_t \quad (9)$$

Substituting Eqns. (7) & (8) in Eqn. (6) and solving for F_c gave Eqns. (10) and (11).

$$F_c = q\,(aV_t - V_1) + f\,F_c \quad (10)$$

$$F_c = \frac{q(aV_t - V1)}{1-f} \quad (11)$$

Threshing power was obtained by multiplying the threshing force (F_c) by velocity (V_t), (Olaoye *et al.*, 2011) using Eqn. (12).

$$P_c = F_c V_t = \left(\frac{q(aV_t - V_1)}{1-f}\right) V_t \quad (12)$$

Where, q = feed rate (kg s^{-1}), V_2 = speed of crop as it exits off the cylinder tip (m s^{-1}),

V_1 = speed of the feed as it enters the cylinder (m s^{-1}); a = empirical coefficient,

f = coefficient of friction, and V_t= cylinder tip linear velocity (ms^{-1}).

The exit velocity of the threshed crop (V_2) just at the cylinder tip is usually equal to the linear speed (V_t) of the cylinder (Chavoshgoli *et al.*, 2019) and V_1 is very small nearer to zero when it reaches at the cylinder for manual feeding, i.e., $V_2 = V_t$ and $V_1 \approx 0$.

Value of ″a″ is between 0.70 and 0.85 for cylinder length of 0.80 m, grain moisture contents between 15.00% and 25.00% (db), and feed rate of 3.50 kg s^{-1}. The value of ″f″ is between 0.65 and 0.75 for rasp bar and between 0.70 and 0.80 for peg type cylinder (Mohtasebi *et al.*, 2006). As the length and moisture were similar, an average of the range was taken and then extrapolated for the level of our feed rate that resented in 0.78 for ″a″. In terms of "f" average value of both conditions (0.73) was directly used as our design is composed of both types of the cylinder elements.

The power given by equation (12) was not enough for threshing, hence, it needs additional power to overcome the air resistance against rotation of the cylinder and friction forces in bearings, and this additional power was estimated using Eqn. (13) (Chavoshgoli *et al.*, 2019).

$$P_r = AV_t + BV_t^3 \quad (13)$$

Where, P_r =power to overcome resistances to the cylinder rotation (w), AV_t = power to overcome force of bearing friction (w), and BVt^2 = power to overcome air resistance (w).

″A″ and ″B″ are coefficients of the threshing cylinder physical properties as described in Mohtasebi *et al.* (2006), and have values of 0.85 to 0.90 N per 100 kg mass of rasp bar cylinder and 5.00 to 5.50 N per 100 kg mass of peg types cylinder for ″A″; and 0.065 Ns^2 m^2 per m length of rasp bar cylinder of 0.55 m diameter and 0.045 Ns^2 m^{-2} per m length of peg type of 0.55 m diameter for ″B″.

Values of A and B were extrapolated based on the given criterion and values, for the composite cylinder type, with given total mass and length of 0.80 m and diameter of 0.38 m. The mass of the composite cylinder was calculated from densities and dimensions of the raw material used for each component parts, i.e., Galvanized Iron sheet metal rolled, round iron pipes and wire used for rasp bars, round iron pegs, flat spikes, wire loops, shaft and pulleys materials. The weight of the parts was calculated using Eqn. (14).

$$M_C = \rho wlt + \rho\pi r^2 h \quad (14)$$

Where, ρwlt = weight of the raw materials item with rectangular dimension; $\rho\pi r^2 l$ = weight of the raw materials item with circular (cylindrical) dimension; M_C = total weight of the threshing cylinder (kg); ρ = density of the cylinder part material items (kg m^{-3}); w, l and t, width, length, thickness of flat raw material items used, respectively (m); and r and h are radius and height of circular raw material items (m). The first term of the above equation just after the equal sign stands for rectangular/flat shaped elements and the second term stands for cylindrical elements of round/circular shape. The threshing cylinder total mass was found to be 35.00 kg.

The total power required by threshing unit is the sum of the power needed for crop threshing as calculated by equations (12) and the power to overcome frictions forces as calculated in equation (13) that was added using Eqn. (15).

$$P_s = P_c + P_r = V_t\left(\frac{q(aV_t - V_1)}{1-f}\right) + (AV_t + BV_t^3) \quad (15)$$

2.2.4. Design of the cylinder pulleys

Diameters of the pulleys were determined according to Khurmi and Gupta (2005) from the speed ratio of the driving and driven pulleys (Eqn. 16). The rpm of the larger pulley was the design speed of the cylinder and it was taken 500 rpm. The speed of the smaller pulley is simply the rated speed of the selected engine.

$$R_p = \frac{N}{n} = \frac{D}{d} \quad (16)$$

Where, R_p = pulley ratio; n = cylinder shaft rpm, N =engine shaft rpm; D = larger pulley diameter (m); and d = smaller pulley diameter (m).

Diesel engines with a low-speed of 1400 rpm was found in local markets and considered for power source of the thresher. This engine speed should be reduced to the selected 500 rpm of the threshing cylinder shaft from which the pulley ratio of 2.80 was calculated. The pulley diameter range of 114 to 140 mm was indicated from the A-section v-belt drive standard Table for the fast pulley turning at the speed of 1400 rpm (Bhandari, 2010). Accordingly, the average diameter of 125.00 mm was selected from the standard pulleys table resulting in the larger pulley diameter of 350.00 mm.

The centre distance of the two pulleys was determined following the general centre distance principle of D < C < 3(D +d) suggested by Khurmi and Gupta (2005) and Eqns. (17) to (19) were used to determine centre distance and belt length.

$$C = \frac{b+\sqrt{b^2-8(D-d)^2}}{8} \quad (17)$$

$$b = 2L_e - \pi(D+d) \quad (18)$$

$$L_e = 2C + \frac{\pi}{2}(D+d) + \frac{(D-d)^2}{4C} \quad (19)$$

Where, D = larger pulley diameter (mm), d = smaller pulley diameter (mm), C = distance between the centres of the pulleys (mm), and L_e = effective length of the v-belt (mm).

The centre distance of 570.00 mm was determined based on the general criteria of D < C < 3(D+ d) and the space available on the frame for installation. The belt with a standard length of 1910.00 mm obtained nearest to the calculated value was selected from the A-section v-belt rating. The contact angles between the belt and the pulleys were calculated according to Khurmi and Gupta (2005) with Eqns. (20) and (21); that resulted in 203° and 157° for larger and smaller pulleys, respectively.

$$\theta_D = 180^o + 2sin^{-1}\frac{(D-d)}{C} \quad (20)$$

$$\theta_d = 180^o - 2sin^{-1}\frac{(D-d)}{C} \quad (21)$$

Where, θ_D and θ_d were contact angles of the larger and smaller pulleys, respectively.

2.2.5. Design of cleaning unit

The blower was designed to discharge a blast of cleaning air through the threshing outputs under the concave. It requires the air flowing at higher velocity than the terminal velocity of the chaffs but lower than the terminal velocity of the grains. Sabar *et al.* (2020) reported terminal velocities of from 6.18 to 7.99 m s^{-1} for sorghum grains moisture content ranging from 8.70% to 21.80% (wb) and said cleaning air velocity should be some points below the minimum terminal velocity. The optimum blower air velocity of 4.68 m s^{-1} was reported for maximum sorghum cleaning efficiency of 96.40 % that decreased to 94.40% when velocity increased from 4.68 m s^{-1} to 7.33 m s^{-1} (Simonyan *et al.*, 2006). A maximum sorghum cleaning efficiency of 98.6% was also reported at air speed of 4.66 m s^{-1} for sorghum that decreased to 98.2% when air speed increased to 7.82 m s^{-1} (Yayock *et al.*, 2020). Hence, air speed 4.67 m s^{-1} was used averaging the two speeds reported for maximum sorghum cleaning efficiency since grain moisture were within similar range in all cases. The rate of airflow desired for cleaning could be determined from the concentration of the material entrained by the air (μ) which is defined as the ratio of the impurity removal to that of air mass flow rate and its value ranges from 0.20 to 0.30 while the airflow rate required to remove the impurities can be calculated using Eqn. (22) according to Bosoi *et al.* (1990).

$$Q_A = \frac{G_a}{\rho_a} = \frac{G_m}{\mu\rho_a} \quad (22)$$

Where, Q_A = air flow volume ($m^3 s^{-1}$); G_a = air mass flow rate (kg s^{-1}); ρ_a = air density (1.20 kg m^{-3}),

G_m = impurity to be removed (kg s^{-1}), and μ = concentration ratio of G_m to G_a.

The Q_A value of 0.185 $m^3 s^{-1}$ was calculated using equation (22) and taking G_m as 8% for sorghum (El-Fakhrany *et al.*, 2017). The actual volumetric air flow rate (Q_A) required at air outlet can be estimated from air velocity (V_a), and cross-sectional area of the air stream (Chavoshgoli *et al.*, 2019) as given by Eqn. (23).

$$Q_A = V_a A = V_a dW \quad (23)$$

However, the theoretical air flow rate has low flow efficiency of 30% and could be corrected using Eqn. (24) (Muhammad *et al.*, 2013).

$$Q_T = \frac{Q_A}{0.3} = \frac{V_a dW}{0.3} \quad (24)$$

Where, Q_T = theoretical flow rate ($m^3 s^{-1}$); Q_A = actual flow rate ($m^3 s^{-1}$); V_a = cleaning air velocity (m s^{-1}); dW =A= blade area (m^2); d = depth of air stream (m), and W = width of air stream (m). Hence, Q_T value of 0.617 $m^3 s^{-1}$ was obtained from Eqn. (24).

The width of the airflow stream was the same as the width of the material flow stream under the concave. Hence, it is equal to the effective material underflow length of 550 mm. The blower air inlet radius was calculated assuming that the blower housing was airtight and had no air leaks, hence air entering and leaving the blower house was equal, and Eqn. (25) was used to calculate it (Zewdu Abdi, 2007).

$$Q_{in} = Q_A = \pi r_i^2(\omega r_i) \quad (25)$$

Where, r_i = radius of air inlet (m), and ω = angular velocity of the blower shaft (rad/s).

The blower rpm is determined from the suggested cleaning air velocity, blower shaft rpm and blower blade tip diameter. The blower shaft running at a maximum speed of 1000 rpm as suggested for cereal cleaning (Bosoi *et al.*, 1990). This suggestion resulted with the speed ratio value of 2 between the blower shaft and threshing cylinder pulley to rotate at 500 rpm using Eqn. (16).

The minimum diameter of grove pulley available as per the standard table was 75.00 mm for A-section v-belt at pulley speed of 1000 rpm and 0.78 kW rated power that leads to 150.00 mm diameter for the driver pulley on the cylinder shaft based on the pulley ratio indicated above. The centre distance between the driving and driven pulleys of the blower was taken 450.00 mm based on operation conveniency and available space on the frame. The belt length calculated for the blower derive system indicated 1250 mm resulting in contact angles of 160° and 200° on the smaller and larger pulleys, respectively. The groove angle of the pulleys of 38° was selected from standard Table A-section v-belts.

The blower blade tip diameter was determined from the selected cleaning air velocity at the blower outlet and the rpm of the blower shaft. The ratio of the blower blade internal diameter or the air inlet diameter (d) to the blade tip diameter (D) ranges from 0.40 and 0.70, i.e., $0.40 < d/D < 0.70$, according to ASME (Suleiman *et al.*, 2016). The ratio d to D, of 0.60 was used in this design, hence, the internal diameter that equal to the inlet diameter ($2r_i$ = 160 mm), then the external diameter, D = d/0.60 = 160.00 mm/0.60. Accordingly, D = 260.00 mm and d = 160 mm were used in the design.

Impeller absolute velocities at inlet (V_i) and outlet (V_o) were calculated using Eqns. (26) and (27), respectively (Zewdu Abdi, 2007).

$$v_i = \frac{\pi dN}{60} \quad (26)$$

$$v_o = \frac{\pi DN}{60} \quad (27)$$

Where, v_i = impeller internal velocity (m/s), v_o = impeller external velocity, and N = blower shaft rpm (1000).

Tangential components of absolute air velocities were estimated using Eqns. (28) and (29) (Muhammad *et al.*, 2013).

$$v_2 = \frac{Q_A}{\pi D b_2} \quad (28)$$

$$v_1 = \frac{Q_T}{\pi d b_1} \quad (29)$$

Where, d = impeller internal diameter (m); D = impeller external diameter (m), b_1 = width of the blades internal side (m); b_2 = blade external side width. But b_1 and b_2 were taken equal for rectangular blade.

The velocities, v_1 and v_2 indicate tangential components of absolute velocities, and v_2 could be approximated as 20 % of the peripheral velocity of the impeller tip (Muhammad *et al.*, 2013). The power required to operate the blower was computed as the sum of power needed to rotate the blower blades with its shaft and pulley, and the power required to develop the desired pressure head differences to create the necessary airflow rate. The power required to rotate 3.60 kg measured weight of blower blades and its pulley on the shaft assuming no airflow (P_{na}) was calculated using equation (5). Inserting the values, the power needed to rotate the blower with no airflow was found to be 0.112 kW. The power required to suck and blow the mass of the air stream at a given velocity to remove impurities was calculated using Eqn. (30) (Korpella, 2011; Sale *et al.*, 2017).

$$P_b = \frac{\rho_a Q_T g H_t}{\eta} \quad (30)$$

Where, P_b = power required by the blower (W), ϱ = density of air (1.20 kg m^{-3} at 20 °C),

Q_T = theoretical volume of air discharge rate ($m^3 s^{-1}$), g = acceleration due to gravity (9.81 m s^{-1}), H_t = total pressure head (m), and η = power efficiency of blower, and it varies between 0.69 and 0.75 (Frank, 1997).

Total pressure head is sum of dynamic and static pressure heads (Frank, 1997) as Eqn. (31).

$$H_t = h_d + h_s \quad (31)$$

The dynamic head of the blower pressure was determined from Bernoulli's principle as given by Eqn. (32) (Schobeiri, 2010).

$$h_d = \frac{V_a^2}{2g} \quad (32)$$

Where, h_d = dynamic pressure head (m), V_a = air flow velocity (m s^{-1}) and g = gravitational acceleration (m•s^{-2});

Hence, h_d was calculated using Eqn. (32) to be 1.11m. The static pressure head depends on the resistance of air and grain property was calculated by Eqn. (33) as used in Bosoi *et al.* (1990).

$$h_s = \frac{(1-k^2)h_d}{k^2} \quad (33)$$

Where, k = coefficient, and is 0.80, and h_s = static pressure head (m).

Inserting the values of h_d and k in Eqn. (32), static head h_s found to be = 0.63 m. Substituting the values of h_d and h_s in Eqn. (30), H_t was estimated to be 1.74. Inserting the value of H_t in Eqn. (30), the power needed to blow the air (P_b) was calculated and found to be 0.03kW.

The total blower power (P_{fn}) = P_{nl} + P_b = 0.112kW + 0.025kW = 0.137 kW. Hence, the total power required to operate the prototype threshing unit (P_t) was 2.718 kW. The total power required to effect threshing and cleaning was calculated using Eqn. (34).

$$P_T = P_t + P_{fn} = (P_u + P_c + P_r) + P_{fn} \quad (34)$$

Inserting the values in Eqn. (34), P_T was estimated to be 2.86 kW.

Tensions (forces) in the belts were determined using equations adapted from BANDO Chemical Industry (2018) standard belt design manual as presented below with Eqns. (35) to (38).

$$T_c = m.{v_b}^2 \quad (35)$$

$$V_b = \frac{\pi dN}{60} \quad (36)$$

$$m = \rho.A \quad (37)$$

Where, T_c = centrifugal tension (N); m = specific mass of the belt (kg/m) = 0.12 kg m^{-1} for rubber,

V_b = belt velocity (m s^{-1}); d = smaller pulley diameter (m); N = rpm of smaller pulley (rpm).

ρ = density of the belt material (kg m^{-3}), and A = cross-sectional area of the belt (m^2).

Belt tension ratio could be computed with help of Eqn. (38).

$$\frac{T_1}{T_2} = e^{\mu\theta cosec\beta} \quad (38)$$

Where, T_1 = tight side belt tensions (N); T_2 = slack sides belt tensions (N); μ = coefficient of friction between belt and grooved pulley surface; θ = arc of contact on the larger pulley (radian); β = half of the pulley grove angle (degree), and e = base of natural logarithms (2.71828).

The coefficient of friction between pulley material and belt (μ) was taken as 0.30 (Khurmi and Gupta, 2005) whereas the density of belt material (rubber belt) was taken as 1250 kg m^{-3} and the working stress of 2.26 MN/m^2 was used from power transmission belts' standard table. The maximum allowable belt tension was estimated from Eqn. (39).

$$T_{max} = \sigma.A \quad (39)$$

Where, σ = maximum stress of rubber belt (Nm^{-2}), and A= belt cross-sectional area (m^2)

Effective tension (T_e) was calculated using Eqn. (40) or Eqn. (41).

$$T_e = T_1 - T_2 \quad (40)$$

$$\text{OR } T_e = \frac{1000P_t}{V_b} \quad (41)$$

Where, P_t = Power transmitted to the driven shaft (kW), V_b = belt velocity (m s^{-1}); P_d = design power (kW), and T_1=tight side tension (N).

The torque on a shaft was calculated using Eqn. (42).

$$T_q = (T_1 - T_2)\, r = T_e.r \quad (42)$$

Where, r = radius of the pulley on the shaft (m).

Power transmitted by the belt was estimated from Eqn. (43).

$$P_t = T_q\omega = T_e\omega r = (T_1 - T_2)V \quad (43)$$

The total power required for threshing unit (P_t) is then sum of all components added as Eqn. (44)

$$P_t = P_u + P_c + P_r = \left[\frac{2\omega r M_C}{75}\left(g + \frac{v_t^2}{r}\right)\right] + \left[\left(\frac{q(aV_t - V_1)}{1-f}\right)V_t\right] + [AV_t + BV_t^3] \quad (44)$$

The design power (P_d) was obtained by multiplying the calculated total power (P_t) with the service factor (SF), where its recommended value is 1.20 for small scale machinery as indicated in BANDO Chemical Industry (2018). The total design power was calculated using Eqn. (45).

P_d = SF x P_t (45)

Hence, substituting values, P_d = 1.2 x 2.844 kW = 3.43 kW.

Number of belts required to transmit the power to the cylinder shaft is given by Eqn. (46).

$$N_b = \frac{P_d}{P_c} \quad (46)$$

Where, N_b = number of belts; P_d = design power (kW), and P_c = correction power rating (kW).

Substituting values, $N_b = \frac{3.43kW}{3.33\ x\ 0.8} = 1.30 \cong 2$ belts of A-section.

2.2.6. Determination of shaft diameter

The minimum diameter of a milled steel shaft that withstands all applied forces, torques, moments, fatigue, etc. (Figure 4) with little or no axial load can be determined using Eqn. (47) (Aung *et al.*, 2019).

$$d^3 = \left(\frac{16}{\pi\tau_{max}}\sqrt{(K_b M_b)^2 + (K_t M_t)^2}\right) \quad (47)$$

Where, d = shaft diameter, mm; M_t = torsional moment, N mm; M_b = bending moment, N mm; K_t, K_b = combined shock and fatigue factor applied to bending and torsional moment respectively; K_b = 1.2 to 2.0; K_t = 1.0 to 1.5; and τ_{max} = the maximum shear stress 55 MPa for milled steel shaft without the key way and 40 MPa for the shaft with the key way.

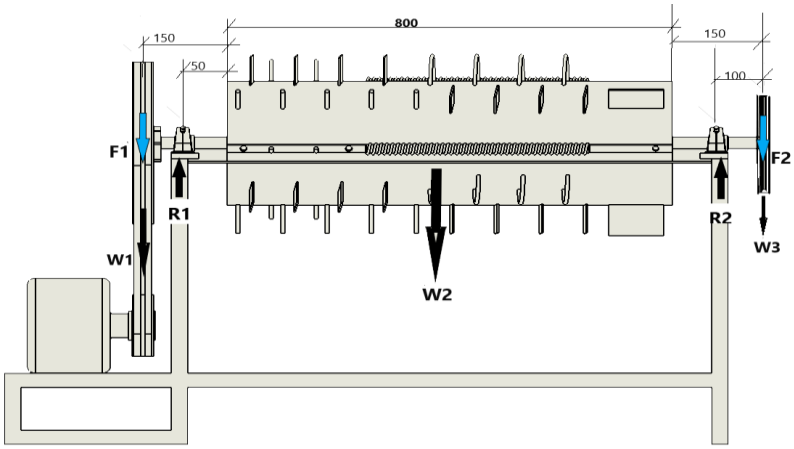

Figure 4. Components of the forces acting on the threshing cylinder shaft.

The torsion on a shaft was calculated from the total power (Eqn. (44)). Vertical forces were determined from the weights of the components and belt tensions. Torsional moment M_t can be calculated with Eqn. (48) (Azharuddin *et al.*, 2016).

$$M_t = \frac{60P}{2\pi N} \quad (48)$$

Where, P = power required to drive threshing (w), and N = speed of the shaft (rpm).

The magnitudes of the forces acting on the cylinder shaft indicated in Fig.4 were determined from the summation of forces using Eqn. (49) and summation of the bending moments using Eqn. (50).

$$\sum F_i = 0 = F_1 + W_1 + W_2 + F_2 + W_3 + R_1 + R_2 \quad (49)$$

The bending moments on the shaft at about R_1 and R_2 were calculated using Eqn. (50).

$$\sum M_b = \sum F_i . X_i = 0 \quad (50)$$

The resultant bending moment was calculated using Eqn. (51) (Azharuddin *et al.*, 2016).

$$M_b = \sqrt{(M_H)^2 + (M_V)^2} \quad (51)$$

Where, M_H = maximum bending moment on horizontal (Nm), M_V = maximum bending moment on vertical plane (Nm), and Mb = resultant bending moment (Nm).

The loads acting on the cylinder shaft and a summary of their calculated values used to determine shaft diameter are given in Table 1.

Table 1. Calculated values of load acting on the shaft to determine shaft diameter.

Loads	Parameters	Values
F_1	Total belt tension of the cylinder drive	335.25 (N)
W_1	Weight of the driven cylinder pulley	10.80 (N)
R_1	Reaction force at left side support	548.76 (N)
W_2	Total weight of the cylinder at the centre of gravity	338.45 (N)
R_2	Reaction force at right side support	180.29 (N)
F_2	Total belt tension of the blower dive	38.68 (N)
W_3	Weight of the blower driver pulley on the cylinder shaft	5.89 (N)
M_b	Resultant bending moment	162.26 (Nm)
M_t	Total torsional moment	54.65 (Nm)

Considering k_b =1.5 and k_t =1.25, and substituting values of moment and torque in Eqn. (47), the diameter of the shaft was determined as follows

.

$$d^3 = \frac{16}{3.14x55x10^6 Nm^{-3}}\sqrt{(1.5x162.26Nm)^2 + (1.25x54.65Nm)^2}$$

$d = 0.0286\ m \cong 0.03m = 30.00\ mm$ was used

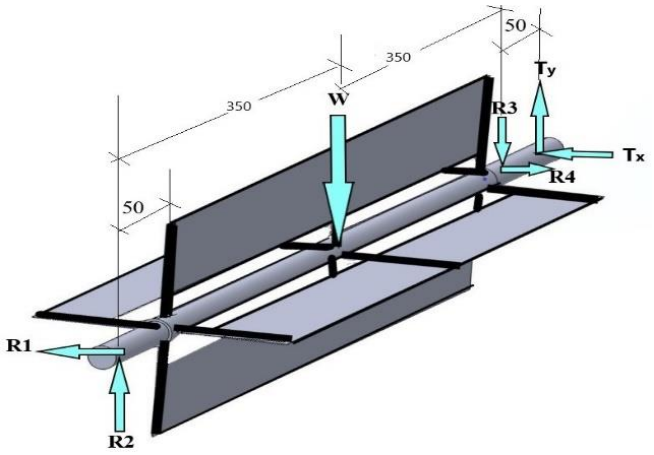

Figure 5. loads acting on the blower shaft.

The loads acting on the blower shaft (Fig. 5), bending and torsional moments, and shaft size were calculated in similar ways using equations (47) to (51) that resulted in milled steel shaft diameter of 18.32 mm and the standard size of 20 mm was used.

2.3 Manufacturing and Prototype Functionality Test

2.3.1. Location of the study area

The study was conducted at Fadis Agricultural Research Centre (FARC) in Eastern Oromia, Ethiopia. The designed thresher was manufactured in engineering workshop according to the design and given specifications. The prototype produced was tested for its functionality on the research site of the centre using the selected sorghum variety produced on the research station.

2.3.2. Test materials and facilities

The prototype thresher was tested using the *Gubbiye* sorghum variety. *Gubbiye* variety was selected for the testing because of its relatively the hardest threshing properties, particularly for its known large grain ratio remaining with glumes and high grain remaining on the straws among the available varieties. It was selected based on consultations an oral recommendations of sorghum breeders and farm management experts. Digital tachometer, digital calliper, oven dry and analytical balance were some of the laboratory facilities used.

2.3.3. Design and treatments

The thresher was tested at 8.00 mm and 13.00 mm levels of concave clearance factor, feed rates of 0.79, 1.18 and 1.58 t/h and cylinder speed factor levels of 400, 500 and 600 rpm while the grain moisture was maintained at 14.51% (wb). The experiment was laid in $2x3^2$ factorial design with 3 replications.

2.3.4. Dependent variables

The data was collected for the dependent variables which include the weight grain entered the thresher at inlet, the unthreshed collected from the straws, the damaged grains obtained in the samples of the grain output, the threshed grains collected after passing with the straws and scattering collected, the grain remained in glumes and impurities obtained from the samples taken from of the grain output and the weight of the clean grain obtained per unit run time of the thresher. The data were converted into percents using Eqns. from (52) to (56) as indicated in Abich *et al.* (2017) and Idris *et al.* (2018).

Threshing efficiency (%) $T_E = \frac{G_i - G_u}{G_i} x100$ (52)

Cleaning efficiency (%) $C_E = \frac{M_i}{M_s} x100$ (53)

Unthreshed grain loss (%) $U_L = 100 - T_E$ (54)

Mechanically damaged grain (%) $D_L = \frac{G_D}{G_C} x100$ (55)

Grains remained with glumes (%) $Q_L = \frac{G_G}{G_C} x100$ (56)

Where, G_i = total grain in the feed (kg); G_u = unthreshed grain collected (kg); Mi = impurity in the output (g); Ms = samples taken from output (g); G_D = damage grain (g), and G_C = sample taken from clean grain (g).

2.3.5. Data analysis

The collected data was organized as per the design and subjected to analysis of variance using GenStat 18th edition statistical software. Ryan/Einot-Gabriel/Welsch multiple comparison test method was used for significance of the mean differences at 95% confidence intervals using the least significant differences (LSD).

3. Results and Discussions

The variance analysis output of the data collected indicated significant (p< 0.001) effect of the treatments for variation of main factors' levels and for variations of the interactions between different levels of involved treatment factors.

3.1 Threshing Efficiency and Unthreshed Grain Loss

The threshing efficiency indicated 98.58% grand mean with the entire means ranging from 96.15% to 99.52% (Table 2) which in other ways indicates unthreshed mean grain loss from minimum of 0.48% to the maximum of 3.85% with grand mean of 1.42%. The minimum efficiency was obtained at 13 mm concave clearance and feed rate of 1.56 t h^{-1} for at speed of 400 rpm while the maximum was recorded at 8 mm clearance, 0.79 t h^{-1} feed and 600 rpm.

Table 2. Means of threshing efficiency as affected by interactions between concave clearance, feed rate and cylinder speed levels.

Concave clearances (mm)	Feed rates (t h^{-1})	Interaction means at different drum speed		
		400 rpm	500 rpm	600 rpm
8.00	0.79	98.91^{defghi}	99.33^{jkl}	99.52^{l}
	1.18	98.77^{cdefg}	$99.00^{efghijk}$	99.14^{fhijkl}
	1.56	98.37^{c}	98.69^{def}	$98.98^{deghijk}$
13.00	0.79	97.84^{b}	$98.93^{defghij}$	99.36^{ikl}
	1.18	97.77^{b}	98.52^{cd}	98.83^{cdefgh}
	1.56	96.15^{a}	97.69^{b}	98.67^{cde}

The mean efficiency recorded is far greater than the threshing efficiency range of 87.28 % to 95.30% reported (Takkalign Badad, 2021) for the IITA multi-crop modified for Muyra sorghum variety within speed range of 500 to 900 rpm, 0.60 to 1.20 t h^{-1} feed rates and 13 to 23 mm concave clearance levels.

3.2 Cleaning Efficiency

The means cleaning efficiency was ranged from 93.46% to 97.83% indicating grand mean of 95.43%. The means were increased from the minimum mean at the lowest speed and the maximum feed rate to the maximum at the highest speed for the minimum feed level. It was increasing with increase of cylinder speed and decreasing with increase in feed rates with no significant effect for variation in concave clearance levels. The cleaning efficiency increase from 83.07% at fan speed of 770 to 89.57% at increased speed of 910 rpm reported for sorghum (Ermias Melkamu, 2019) at constant feed of 12 kg min^{-1} (0.72 t h^{-1}) is far lower than our finding with doubled feed rate and reduced speed.

3.3. Damaged Grain Loss

Significantly different means of damage grains was observed as affected by variation of the factors' levels and the interactions of the factors' levels for which the entire means ranged from 0.25% % to 1.07% with grand mean of 0.77% (Table 3). The means were increasing with increase of cylinder speed and decreasing with increase in concave clearance and feed rates. The means of mechanical damage recorded were entirely lower than the sorghum grain damage range of 2.25 to 3.73% reported (Sale *et al*., 2016) with grain moisture increase of 11% to 15% (wb) and decrease of feed rate from 300 to 180 kg h^{-1}.

Table 3. Percent of damaged grains as affected by entire interactions of treatments' levels.

Concave clearances (mm)	Feed rates (t h^{-1})	Interaction means at different drum speed		
		400 rpm	500 rpm	600 rpm
8.00	0.79	0.81^{fg}	0.99^{hi}	1.07^{j}
	1.18	0.67^{def}	0.76^{ef}	1.02^{i}
	1.56	0.33^{ab}	0.58^{cde}	0.85^{fg}
13.00	0.79	0.51^{bcd}	0.84^{fg}	0.98^{gh}
	1.18	0.33^{ab}	0.47^{bcd}	0.71^{ef}
	1.56	0.25^{a}	0.39^{abc}	0.56^{de}

3.4. Grains Remained with Glumes

The test result indicated means of grains remained with glumes ranging from minimum of 2.02% to the maximum of 4.15%, with grand mean of 3.16%, with and respectively (Table 4). Increasing of clearance from 8 to 13 mm increased percent of grains in glumes from 3.61% to 4.15% at 400 rpm and increase of speed from 400 to 600 rpm reduced grains in glumes from 4,15% to 2.25%.

Table 4. Means of grains remained with glumes for clearance and cylinder speed interactions.

Concave clearance levels	Interaction means at different drum speed		
	400 rpm	500 rpm	600 rpm
8.00 mm	3.61^{c}	2.98^{b}	2.25^{a}
13 mm	4.15^{d}	3.48^{c}	2.48^{ab}

The mean maxim of grain remained with glumes was recorded at minimum speed of 400 rpm and 13 mm concave and this is nearly a third of the 9.33% reported by Takkaling Badada (2018) for the modified IITA multi-crop thresher on the *Muyra* sorghum variety.

4. Conclusion

Testing of the prototype showed a high average threshing efficiency of 98.58%, with a minimal average grain damage of 0.77% and a tolerable average of 3.16% in terms of grains remaining in the glumes. Since the *Gubbiye* sorghum variety is characterized by its challenging threshing properties, this test result implies that the thresher has good potential for use to thresh efficiently this variety as well as other sorghum varieties in the country. Further evaluation of the thresher at different combination levels of concave clearance, cylinder speeds, feed rates and grain moisture content treatment factors are recommended to identify the best combination of operational settings adjustment that reduce the grains remaining in their glumes.

5. References

Abdulaziz Teha, Takkalign Bedada, Jamal Nur, Ibsa Aliyi and Kibret Ketema. 2020. Pre-extension demonstration and evaluation of engine-driven sorghum thrasher in the selected AGP-II districts of Harari Region and Dire Dawa administration. *Food Science and Quality Management,* 97: 29–32.

Abich, S.O. 2018. Optimization of threshing performance of a spike tooth sorghum threshing unit. MSc Thesis, Egerton University, Kenya. Pp. 80.

Abich, S.O., Ngunjiri, G.M. and Njue, M.R. 2017. Effect of cylinder diameter and peripheral speed on the performance of a sorghum thresher. *IOSR-Journal of Agriculture and Veterinary Science,* 10(8): 44–50.

Ali Mohammed and Abrham Tadesse. 2018. Review of major grains postharvest losses in Ethiopia and customization of a loss assessment methodology. USAID/Ethiop Agriculture, knowledge Learning, Documentation and Policy Project. Addis Ababa, Ethiopia.

https://pdf.usaid.gov/pdf_docs/PA00TGW5.pdf. Accessed on 17 May 2022.

Ali, K., Zong, W., Tahir, H., Ma, L. and Yang, L. 2021. Design, simulation and experimentation of an axial flow sunflower-threshing machine with an attached screw conveyor. *Applied Science,* 11(14): 1–13.

Aung, L., Theint, E. and Win, H. 2019. Structural analysis of shafts and bearings for paddy thresher. *Iconic Research and Engineering Journals,* 3(1): 385–390.

Azharuddin, K., Mir, S., Narasimhan, M. and Kumar, G. 2016. Design and fabrication of sunflower seed extracting machine. *International Journal of Latest Technology in Engineering, Management and Applied Science,* 5(6): 90–97.

BANDO Chemical Industry Ltd. 2018. Power Transmission Products: V-Belt Design Manual, Version 2018. https://portalimages.blob.core.windows.net/products/pdfs/syofijri_Bando-Belt-Product-Overview.pdf. Accessed on 19 February 2021.

Bosoi, E.S., Verniaev, O.V., Smirnov, I.I. and Sultan, E.G. 1990. Theory, Construction and Calculations of Agricultural Machines. Oxonian press, London. Pp. 810.

Chavoshgoli, E., Abdollahpour, S. and Ghasemzadeh, H. 2019. Designing, fabrication and evaluation of threshing unit for edible sunflower. *Agricultural Engineering International: CIGR Journal,* 21(2): 52–58.

CSA (Central Statistical Agency). 2020. The federal democratic republic of Ethiopia central statistical agency agricultural sample survey 2019/20. Report on area and production of major crops. Statistical Bulletin, 587. Addis Ababa, Ethiopia. Pp. 137.

CSA (Central Statistical Agency). 2021. The federal democratic republic of Ethiopia central statistical agency agricultural sample survey 2020/21. Report on area and production of major crops. Statistical Bulletin, 590. Addis Ababa, Ethiopia. Pp. 143.

El-Fakhrany, W.B., Shalaby, S.A. and El-Balkimy, W.M. 2017. Developing a unit for chaff bagging during threshing. *Journal of Soil Science and Agricultural Engineering,* 8(2): 49–56.

El-Sharabasy, M.A. and Ali, M.M. 2007. Development of a local threshing machine suits for threshing black seed (nigella sativa). *Misr Journal of Agricultural Engineering,* 24(4): 699–724.

Ermias Melkamu. 2020. Development of a motor driven sorghum thresher. MSc Thesis, Bahir Dar University, Ethiopia. Pp. 146.

FAO (Food and Agriculture Organization). 2017. Postharvest loss assessment of maize, wheat, sorghum and haricot bean. A study conducted in fourteen selected woredas of Ethiopia under the project -GCP/ETH/084/SWI. https://www.fao.org/Ethiopia-Baseline_PHL_food_loss assesment_report-v25jan18_003_pdf. Accessed on 16 September 2020.

FAO (Food and Agriculture Organization). 2020. Crops and livestock products. FAOSTAT Database. https://www.fao.org/faostat/en/%3f#data/QCL. Accessed on 15 June 2022.

Frank, P.B. 1998. *Fan Hand Book: Selection, Application and Design*. McGraw Hill Company Inc., New York. Pp. 640.

Husen Abagisa, Takka Tesfaye and Dubbale Befikadu. 2015. Modification and testing of replaceable drum multicrop thresher. *International Journal of Sciences: Basic and Applied Research,* 23(1): 242–255.

Idris, S.I., Mohammed, U.S., Suleiman, M.L. and Sale, N.A. 2018. Modification and performance evaluation of IAR multi crop thresher for sorghum threshing. *BAYERO Journal of Engineering and Technology,* 13(1): 98–108.

Khurmi, R.S. and Gupta, J.K. 2005. *A Textbook of Machine Design*. 14th edition. Eurasia Publishing House PVT. Ltd., New Delhi. Pp. 1251.

Klenin, N.I., Popov, I.F. and Sukun, V.A. 1985. *Agricultural machines: Theory of operation, computation of controlling parameters and the conditions of operation*. Amerind Publishing Co. PVT. Ltd., New Delhi. Pp. 633.

Korpella, S.A. 2011. *Principles of turbomachinery*. John Wiley and Sons Inc., New Jersy. Pp. 467.

Masresha Fetene, Okori, P., Samuel Gudu, Mneney, E.E. and Kasahun Tesfaye. 2011. Delivering new sorghum and finger millet innovations for food security and improving Liveli-hoods in Eastern Africa. International Livestock Research Institute (ILRI), Nairobi, Kenya. Pp. 45.

Mohtasebi, S., Behroozilar, M., Alidadi, J. and Besharat, K. 2006. A new design for grain combines thresher. *International Journal of Agriculture and Biology*, 8(5): 680–683.

Muhammad, U., Abubakar, L., Isiaka, M. and Davies, R.M. 2013. Design and evaluation of a cleaning machine. *Applied Science Report*, 1(3): 62–66.

Olaoye, J.O., Oni, K.C. and Olaoye, M.O. 2011. Computer applications for selecting operating parameters in a stationary grain crop thresher. *Journal of Agricultural Technology,* 7(1): 39–56.

Sabar, S.S., Swain, S.K., Behera, D., Rayaguru, K., Mohapatra, A.K., et al. 2020. Moisture

dependent physical and engineering properties of sorghum grains. *International Journal of Current Microbiology and Applied Sciences,* 9(8): 2365–2375.

Sale, N.A., Muhammed, U.S., Dalha, I.B. and Idris, S.I. 2016. An improved IAR sorghum thresher. *Agricultural Engineering International: CIGR Journal,* 18(3): 119–126.

Sale, N.A., Muhammed, U.S., Gwarzo, M.A. and Idris, S.I. 2017. Modification and performance evaluation of cleaning system for IAR sorghum thresher. *Journal of Engineering and Technology*, 2(2): 90–94.

Samuel Adimasu, Badaso Taye, Wondwossen Tsegaye, Oumar Taha, Mesfin Ketama and Fikadu Chala. 2014. Dissemination, adoption and impacts of multi-crop threshers in Ethiopia: Experience of Sasakawa Global-2000. Technical Report, No. 03. Addis Ababa, Ethiopia. Pp. 49.

Schobeiri, M. 2010. *Fluid Mechanics for Engineers*: *A Graduate Textbook*. Springer, Berlin. Pp. 517.

Simonyan, K., Yiljep, Y. and Mudiare, O. 2006. Modelling the grain cleaning process of a stationary sorghum thresher. *Agricultural Engineering International: the CIGR Ejournal,* 8: 1–17.

Sisay Debebe. 2022. Post-harvest losses of crops and its determinants in Ethiopia: tobit model analysis. *Agriculture and Food Security,* 11(3): 1–8.

Suleiman, M., Obadiah, K. and Atiku, L. 2016. Design of a centrifugal blower for a 400kg rotary furnace. *American Journal of Engineering Research,* 5(10): 181–186.

Takkalign Bedada. 2018. Improvement of IITA multi-crop thresher for sorghum threshing. *International Journal of Pure and Applied Research*, 2(1): 15–26.

Takkalign Bedada. 2021. Improvement of the engine driven sorghum thresher by incorporating grain cleaning system. *The American Journal of Applied Sciences*, 3(6): 1–7.

Yang, R., Chen, D., Zha, X., Pan, Z., Shang, S. 2021. Optimization design and experiment of ear-picking and threshing devices of corn plot kernel harvester. *Agriculture*, 11:1–23.

Yayock, E., Shebayan, J. and Bature, B.J. 2020. Development of a grain cleaning machine for sorghum and millet. *International Journal of Engineering Science Invention,* 9(8): 35–42.

Zewdu Abdi. 2007. Aerodynamic properties of Teff grain and straw material. *Journal of Biosystems Engineering,* 98(3): 304–309.